Chapter 36
Experimental Study of an Active Window for Silent and Comfortable Vehicle Cabins

Malte Misol, Stephan Algermissen and Hans Peter Monner

Abstract The poor sound insulation of windows especially at low frequencies constitutes a severe problem, both in transportation and in the building sector. Due to additional constraints on vehicles or aircrafts regarding energy efficiency and lightweight construction, the demand of light-weight-compliant noise-reduction solutions is amplified in the transportation industry. Simultaneously, in order to satisfy the customer demands on visual comfort and modern design, the relative size of glazed surfaces increases in all sectors. The experimental study presented below considers the feasibility of actively controlled windows for noise reduction in passenger compartments by using the example of an automobile windshield. The active windshield consists of the passive windshield, augmented with piezoceramic actuators and sensors. The main focus of the subsequent work was the development and evaluation of feedforward and feedback control strategies with regard to interior noise reduction. The structural excitation of the windshield was realized by an electrodynamic exciter (shaker) applied at the roof brace between the A-pillars. By this choice it was possible to emulate the structural excitation of the windshield through the car body, induced by coasting and motor-force harmonics. The laboratory setup does not permit the consideration of hydrodynamic and acoustic loads, which might be important as well. However, the experimental results indicate the high noise reduction potential of active structural acoustic control of structure-borne sound that radiates into a cavity.

M. Misol (✉) · S. Algermissen · H. P. Monner
Institute of Composite Structures and Adaptive Systems, German Aerospace Center DLR, Lilienthalplatz 7, 38108, Braunschweig, Germany
e-mail: malte.misol@dlr.de

S. Algermissen
e-mail: stephan.algermissen@dlr.de

H. P. Monner
e-mail: hans.monner@dlr.de

M. Wiedemann and M. Sinapius (eds.), *Adaptive, Tolerant and Efficient Composite Structures*, Research Topics in Aerospace, DOI: 10.1007/978-3-642-29190-6_36,

36.1 State of Technology

The reduction of noise in passenger compartments of vehicles by means of active electronic devices has been a research issue for more than fifty years. In 1953, Olson and May [1] proposed the application of an electronic sound absorber in the vicinity of the passenger's head in order to reduce unwanted sound. More recent publications deal with the reduction of road noise using the car's audio system as actuator for the active noise control (ANC) system. Both feedforward and feedback algorithms are investigated. Sutton et al. [2] developed an active sound control system for automobiles that uses interior loudspeakers to counteract the low-frequency rumble of road noise when driving on typical road surfaces. In a publication of Oh et al. [3] the development of an active feedforward control system for the reduction of road booming noise is described. Four accelerometers were attached to the suspension system in order to detect reference vibration signals, and two loudspeakers were used for the attenuation of the noise near the headrests of the two front seats. Sano et al. [4] developed an active control system for low-frequency road noise in automobiles with the emphasis on cost efficiency. A recent paper by de Oliveira et al. [5] aims to evaluate, both numerically and experimentally, the effect of a feedback controller on the sound quality of a vehicle mock-up excited with engine noise. The controller performance is evaluated in terms of specific loudness and roughness. All of the mentioned publications implement an active noise reduction system by means of anti-sound. However, not many research results have been published in the field of active structural acoustic control (ASAC) for automobile application. Dehandschutter and Sas [6] propose the application of vibration absorbers at the car body. In Weyer et al. [7] active electromechanical absorbers (AEMA) are applied to a car roof for the realization of an ASAC system. The windshield, however, which constitutes an important factor regarding interior noise, has not been considered in former publications dealing with ASAC. The current paper considers the reduction of windshield-vibration-induced interior noise in an automobile passenger compartment by means of ASAC. The achieved results can be considered to be of generic importance also for other traffic carriers such as trains or aircraft.

36.2 Real-Time Control System of the Active Windshield

The sampling rate was set to 1 kHz. Apart from the microphone signal, all in- and outgoing signals were conditioned by low-pass filters of the type Kemo 21 M with a cut-off frequency set to 240 Hz. The piezo-amplifiers of the type E-471 and P-270 from PI were sufficiently powerful to supply the piezoelectric d31-patches with a maximum voltage of 400 V up to the cut-off frequency. For vibration sensing, six accelerometers of the type PCB 356A18 were placed at heuristically optimized positions on the windshield. The sound pressure level (SPL) at different

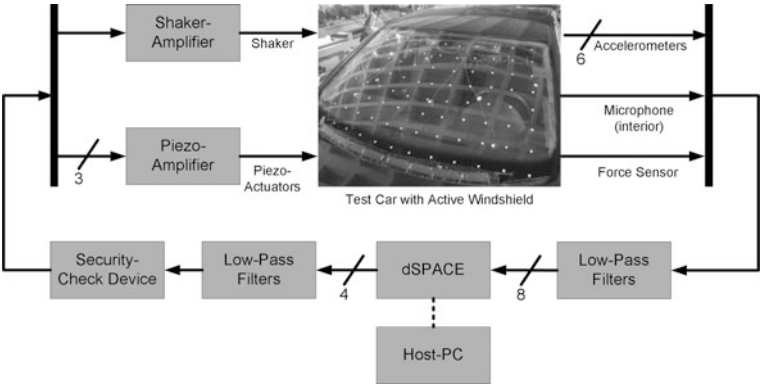

Fig. 36.1 Block-diagram of the real-time control system of the active windshield

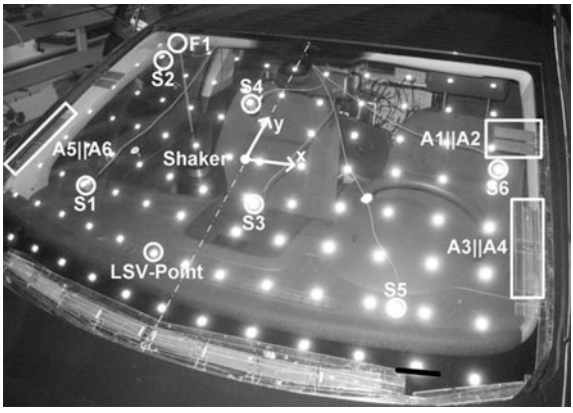

Fig. 36.2 Definition of disturbance force (F), actuators (A) and sensors (S)

positions in the interior of the car was sensed by a PCB 377B02 microphone in combination with a PCB TMS426A01 amplifier. The reference signal for the adaptive feedforward controller was generated from a force sensor placed at the excitation point of the shaker at the roof brace (Fig. 36.1).

36.3 Definition of Sensors and Actuators

Figure 36.2 shows the accelerometer positions (S1–S6) as well as the selected piezo-actuators (A1–A6). The number and position of the sensors was chosen and optimized heuristically by using results from modal analysis and the principle of maximum modal observability. The selection process of the control actuators was guided by the evaluation of control-path frequency-response-functions (FRF). In order to achieve a reasonable trade-off between model complexity and control

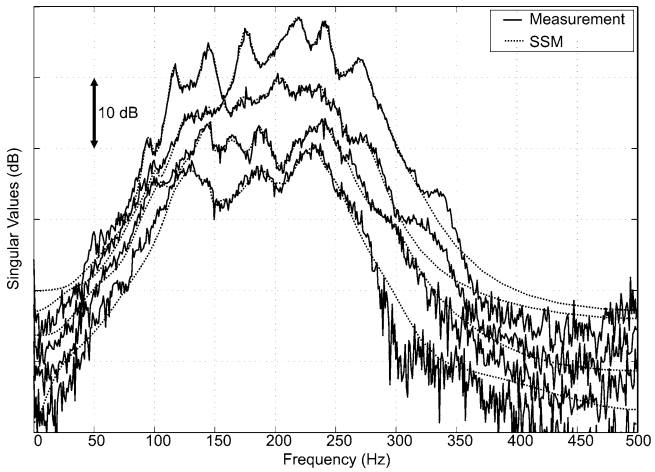

Fig. 36.3 Singular values of control- and disturbance-path FRF-matrix

authority, the number of actuator channels had been restricted to three. A further increase in control authority is obtained by operating adjacent actuators in parallel (Ax||Ay).

In general, it can be stated that the lower actuators 3, 4, 5 and 6 have more authority below 150 Hz and the upper actuators 1 and 2 perform better above 150 Hz. This behavior can be explained by the mode shapes of the windshield system and the corresponding distribution of maximum modal strains. The final choice of actuators was A1||A2, A3||A4 and A5||A6 because in this configuration the singular values of the control path FRF-matrix were largest throughout the controller bandwidth from 0 to 240 Hz.

36.4 Multi-Reference Test and System Identification

A high-precision model of the control system constitutes an important prerequisite for the successful design and implementation of a state-feedback or adaptive feedforward controller. In this study, the SLICOT toolbox [8] was used to identify a discrete-time state-space-model (SSM) for the coarse accelerometer grid (4 inputs, 6 outputs) by means of multiple-reference test data. In order to obtain the global system dynamics in terms of a fine, so-called SLDV-grid (101 points), a subsequent least-squares fit was performed by using the obtained state-space model and measurement data from the scanning laser doppler vibrometer (SLDV). The final result was an augmented state-space system of the same order, but with 101 outputs.

Figure 36.3 compares the singular values of the identified system model with a MATLAB® frequency response data (FRD)-model that had been calculated from measurement data. The agreement of the identified and measured singular values

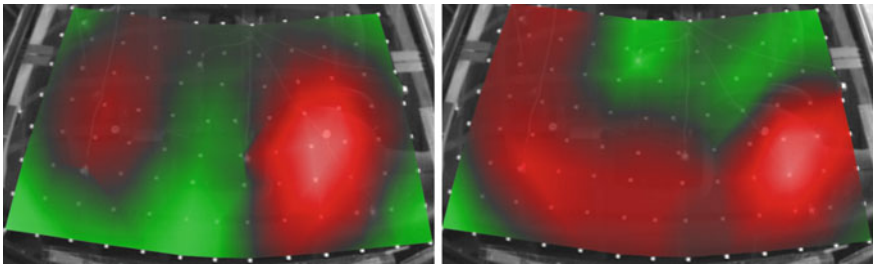

Fig. 36.4 Measured operational velocity shapes at 116 Hz (*left*) and 145 Hz (*right*) without control

within the control bandwidth proves that a numerically efficient and accurate modeling had been achieved with the use of only 60 states.

36.5 Implementation and Evaluation of the Control Algorithms

Modern control strategies are based on the concept of a generalized plant [9]. This method is very generic and provides great flexibility in control strategy formulation. In principle, the designed controllers are broadband within the control bandwidth. However, results of acoustic investigations obtained from road trials and roller test bench experiments emphasize the importance of the second and third eigenfrequency of the windshield system. Due to its importance for the low-frequency interior acoustics, the subsequent discussion is focused on these two structural resonances. In order to allow comparability, the color coding of the operational velocity shapes amplitudes was kept constant for all vibration measurements. The amplitudes are color coded from light green (0 m/s) to light red (9e-4 m/s at 116 Hz and 5e-4 m/s at 145 Hz) (Fig. 36.4).

36.5.1 State-Feedback Control

Figure 36.5 shows the schematic employed for the control design. This formulation follows the generalized plant concept with plant $\mathbf{G_{ext}}$, controller $\mathbf{R}$ and appropriately chosen weighting filters $\mathbf{W_{XYz}}$. The zero-mean, white-noise processes $\mathbf{w_d}$ and $\mathbf{w_r}$ serve as input (process and measurement noise) whereas $\mathbf{z}$ represents the performance output of the generalized plant. The scheme is expressed mathematically in Eqs. 36.1 and 36.2. If $\mathbf{p}$ and $\mathbf{v}$ are identical, the controller minimizes a local performance metric. The global controller is designed with regard to the fine SLDV-grid. In order to enhance the control performance, a model of the disturbance path $\mathbf{G_{11}}$ was included into the generalized plant.

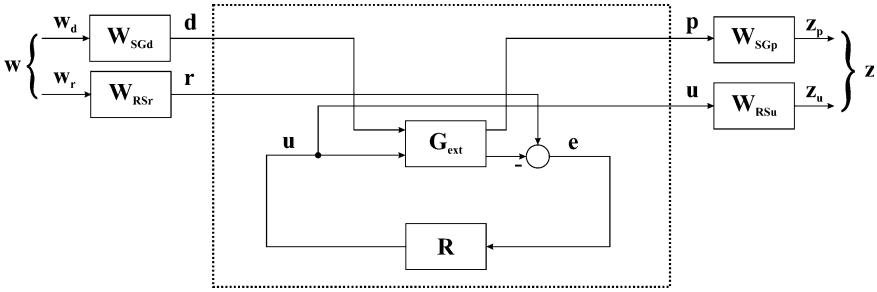

Fig. 36.5 Weighting scheme for FB-controller synthesis

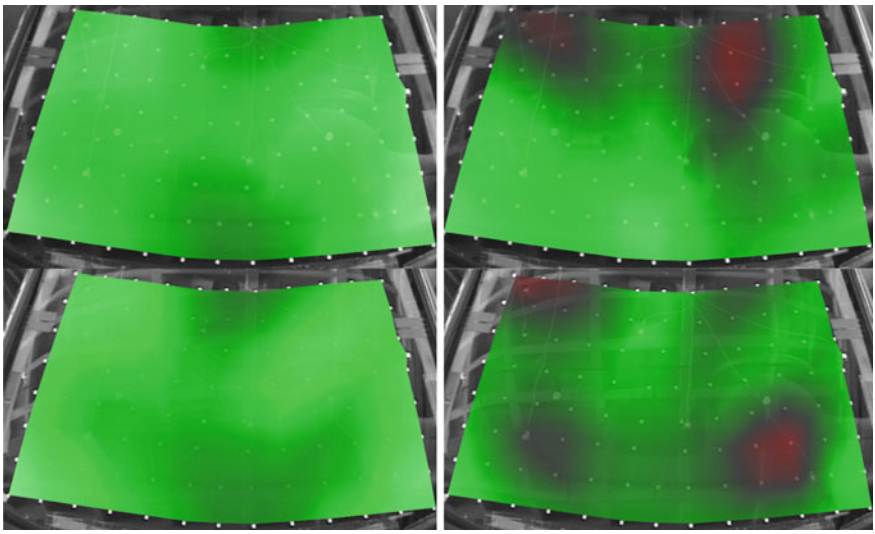

Fig. 36.6 Measured operational velocity shapes at 116 Hz (*left*) and 145 Hz (*right*) with local (*above*) and global (*below*) state-feedback control

$$\begin{bmatrix} \mathbf{z}_\mathrm{p} \\ \mathbf{z}_\mathrm{u} \end{bmatrix} = \begin{bmatrix} \mathbf{W}_\mathrm{SGp}\mathbf{G}_{12}\mathbf{R}\mathbf{S}\mathbf{W}_\mathrm{RSr} & \mathbf{W}_\mathrm{SGp}(\mathbf{G}_{11} - \mathbf{G}_{12}\mathbf{R}\mathbf{S}\mathbf{G}_{21})\mathbf{W}_\mathrm{SGd} \\ \mathbf{W}_\mathrm{RSu}\mathbf{R}\mathbf{S}\mathbf{W}_\mathrm{RSr} & -\mathbf{W}_\mathrm{RSu}\mathbf{R}\mathbf{S}\mathbf{G}_{21}\mathbf{W}_\mathrm{SGd} \end{bmatrix} \begin{bmatrix} \mathbf{w}_\mathrm{r} \\ \mathbf{w}_\mathrm{d} \end{bmatrix} \tag{36.1}$$

With extended plant $\mathbf{G}_\mathrm{ext}$ and sensitivity $\mathbf{S}$:

$$\begin{bmatrix} \mathbf{p} \\ \mathbf{v} \end{bmatrix} = \mathbf{G}_\mathrm{ext} \begin{bmatrix} \mathbf{d} \\ \mathbf{u} \end{bmatrix} = \begin{bmatrix} \mathbf{G}_{11} & \mathbf{G}_{12} \\ \mathbf{G}_{21} & \mathbf{G}_{22} \end{bmatrix} \begin{bmatrix} \mathbf{d} \\ \mathbf{u} \end{bmatrix} \text{ and } \mathbf{S} = [\mathbf{E} + \mathbf{G}_{22}\mathbf{R}]^{-1} \tag{36.2}$$

According to Fig. 36.6, the vibration-reduction performance of local and global feedback control is very similar. One reason for this is the relatively large number of accelerometers compared to the structural wavelengths. This leads to a global vibration reduction even with a local control scheme. The global control would be

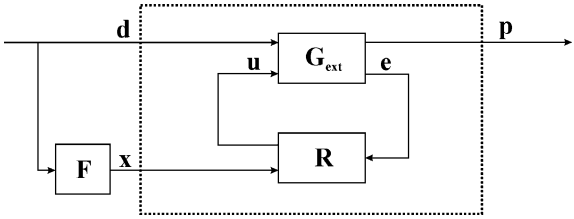

Fig. 36.7 Generalized plant framework for adaptive feedforward control

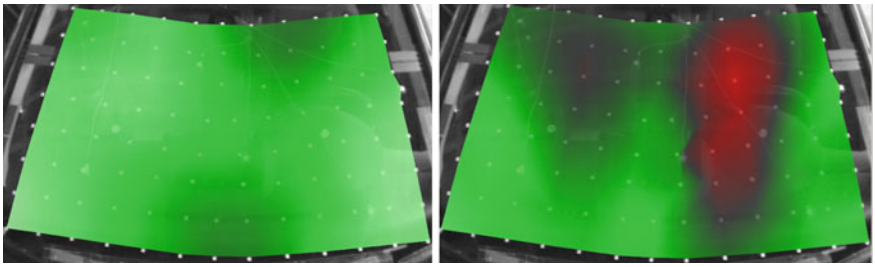

Fig. 36.8 Measured operational velocity shapes at 116 Hz (*left*) and 145 Hz (*right*) with adaptive feedforward control

advantageous if the ratio of structural sensors to control bandwidth was significantly reduced or if a sound power related performance metric was needed. The vibration level reductions of the local feedback controller averaged over the SLDV-grid are 7.54 dB at 116 Hz and 4.36 dB at 145 Hz.

36.5.2 Adaptive Feedforward Control

The implemented feedforward controller is based on finite impulse response (FIR) filters whose coefficients are adapted by means of the well-known filtered-x least mean squares algorithm (FxLMS) [10]. In contrast to the state-feedback control scheme, the FxLMS algorithm performs no post-processing of the sensor signals and hence can only process local information based on the coarse sensor grid ($\mathbf{p} \equiv \mathbf{e}$) (Fig. 36.7).

Adaptive filtering was performed with 200 FIR-filter taps for each control channel, a leakage-factor V = 1 and a normalized step size μ of 0.1 % times the theoretical maximum value. The adaption of the FIR-filter-weights for a single-reference FxLMS with M sensors and K actuators is described by Eq. 36.3.

$$\mathbf{w}(n+1) = \mathbf{w}(n) + \mu \mathbf{X}'(n)\mathbf{e}(n) \tag{36.3}$$

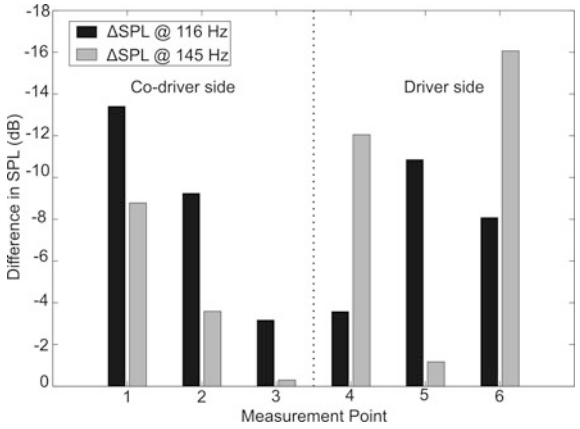

Fig. 36.9 Attenuation of interior sound pressure level (SPL) due to feedforward control

The dimensions of weight-vector **w**, filtered-reference matrix **X**' and error-vector **e** follow from Eq. 36.4. Matrix **X**' is formed by the Kronecker product convolution of impulse response matrix $\widehat{\mathbf{S}}$ and reference signal vector **x**.

$$\begin{aligned} \mathbf{w}(n) &\equiv \left[\, \mathbf{w}_1^T(n) \quad \mathbf{w}_2^T(n) \quad \cdots \quad \mathbf{w}_K^T(n) \,\right]^T \in \mathbb{R}^{KL} \\ \mathbf{e}(n) &\equiv \left[\, e_1(n) \quad e_2(n) \quad \cdots \quad e_M(n) \,\right]^T \in \mathbb{R}^{M} \\ \mathbf{X}'(n) &= \widehat{\mathbf{S}}^T(n) \otimes \mathbf{x}(n) \in \mathbb{R}^{KLxM} \end{aligned} \tag{36.4}$$

Figure 36.8 shows the vibration amplitude with the adaptive feedforward controller. The relative sound pressure levels shown in Fig. 36.9 were measured at six points equally spaced along the **x**-axis at $\mathbf{z} = -0.1$ m (interior).

36.6 Conclusion

Different feedback and feedforward control strategies for the active reduction of interior noise in vehicle cabins have been developed and experimentally approved. A maximum global vibration reduction of 7.5 dB was achieved in the acoustically relevant frequency band containing the second and third eigenfrequency of the windshield system (100–150 Hz). The interior SPL was reduced up to 16 dB.

References

1. Olson, H., May, E.: Electronic sound absorber. J. Acoust. Soc. Am. **25**, 829 (1953)
2. Sutton, T.J., Elliott, S.J., McDonald, A.M., Saunders, T.J.: Active control of road noise inside vehicles. Noise Control Eng. J. **42**(4), 137–147 (1994)
3. Oh, S.H., Kim, H.S., Park, Y.J.: Active control of road booming noise in automotive interiors. J. Acoust. Soc. Am. **111**(1), 180–188 (2002)

4. Sano, H., Inoue, T., Takahashi, A., Terai, K., Nakamura, Y.: Active control system for low-frequency road noise combined with an audio system. IEEE Trans. Speech Audio Process. **9**(7), 755–763 (2001)
5. De Oliveira, L.P.R., Janssens, K., Gajdatsy, P., Van der Auweraer, H., Varoto, P.S., Sas, P., Desmet, W.: Active sound quality control of engine induced cavity noise. Mech. Syst. Signal Process. **23**(2), 476–488 (2009)
6. Dehandschutter, W., Sas, P.: Active control of structure-borne road noise using vibration actuators. J. Vib. Acoust. Trans. ASME **120**(2), 517–523 (1998)
7. Weyer, T., Breitbach, E., Heintze, O.: Self-tuning active electromechanical absorbers for tonal noise reduction of a car roof. In: INTER-NOISE—International Congress and Exhibition on Noise Control Engineering, Istanbul, Turkey. http://elib.dlr.de/52319/ (2007)
8. Favoreel, W., Sima, V., Van Huffel, S., Verhaegen, M., De Moor, B.: Subspace model identification of linear systems in slicot, Technical report, European Community BRITE-EURAM III Thematic Networks Programme NICONET. SLICOT Working Note 1998-6 (1998)
9. Clark, R., Saunders, W., Gibbs, G.: Adaptive structures: dynamics and control. **28**(2) (1998)
10. Kuo, S., Morgan, D.: Active Noise Control Systems: Algorithms and DSP Implementations. John Wiley & Sons Inc., New York (1995)